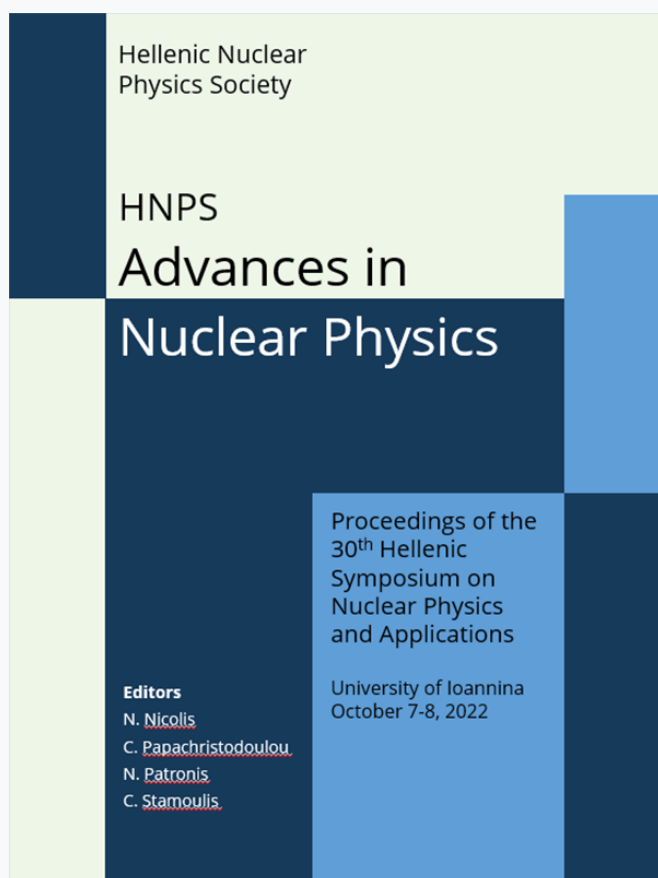


## HNPS Advances in Nuclear Physics

Vol 29 (2023)

HNPS2022



### Assessment of marine radiological impact after an hypothetical nuclear accident in Eastern Mediterranean Sea

*Georgios Eleftheriou, Christos Tsabaris, Konstantinos Tsiaras, Georgios Triantafyllou*

doi: [10.12681/hnpsanp.5097](https://doi.org/10.12681/hnpsanp.5097)

Copyright © 2023, Georgios Eleftheriou, Christos Tsabaris, Konstantinos Tsiaras, Georgios Triantafyllou



This work is licensed under a [Creative Commons Attribution-NonCommercial-NoDerivatives 4.0](https://creativecommons.org/licenses/by-nc-nd/4.0/).

### To cite this article:

Eleftheriou, G., Tsabaris, C., Tsiaras, K., & Triantafyllou, G. (2023). Assessment of marine radiological impact after an hypothetical nuclear accident in Eastern Mediterranean Sea. *HNPS Advances in Nuclear Physics*, 29, 149–155. <https://doi.org/10.12681/hnpsanp.5097>

# Assessment of marine radiological impact after a hypothetical nuclear accident in Eastern Mediterranean Sea

G. Eleftheriou\*, C. Tsabaris, K. Tsiaras, G. Triantafyllou

*Hellenic Centre for Marine Research, Institute of Oceanography, P.O. Box 712, GR-19013 Anavyssos, Greece*

**Abstract** The consequences after a hypothetical nuclear accident at the Akkuyu Nuclear Power Plant in the region of Eastern Mediterranean Sea are presented. The dispersion of the radioactive plume in the sea is simulated applying a regional hydrodynamic/Lagrangian drift model and the radioecological impact is estimated after the release of  $^{137}\text{Cs}$ ,  $^{238}\text{Pu}$  and  $^{131}\text{I}$ . The doses to marine biota and the human inhabitants of the affected regions are presented, while the sensitivity analysis of the results reveal the most vulnerable features of this marine environment.

**Keywords** radionuclides, radiomodelling, dose rate, environmental sensitivity, Akkuyu NPP

## INTRODUCTION

Modelling exercises of radionuclides dispersion in the marine environment are a particularly effective tool for the improvement of radioecological assessments and the development of proper radioprotection strategies [1]. In this frame, several projects aiming to improve the capabilities of simulation radiomodels and decision support systems have been released by the International Atomic Energy Agency (IAEA) [2-5]. For the Mediterranean Sea, radiological models have been developed in regional and local scales focusing on the fate of  $^{137}\text{Cs}$  after the Chernobyl accident [6-9]. Eastern Mediterranean Sea is of particular interest, since it is rapidly affected by climate change and extensive anthropogenic pressures, including radiological threat. More specifically, the recently contracted Nuclear Power Plant (NPP) at the coastal region of Akkuyu, South Turkey, is expected to start its operation in 2023 with one of the total 4 water-water energetic reactors of 1200 MW (VVER1200) electricity generation capacity [10]. To this end, a basin scale 3-D hydrodynamic model coupled with a Lagrangian particle drift model was developed to investigate the dispersion and fate of key radionuclides released from a hypothetical accident and how this will affect the neighboring marine regions [11-12]. In order to include radioactive pollutants typically traced after an accident in nuclear facilities covering a wide range of radioactive half-lives, chemical behavior in the seawater and radioecological characteristics, the dispersion of  $^{137}\text{Cs}$ ,  $^{131}\text{I}$  and  $^{238}\text{Pu}$  was simulated after an instant accidental release into the surrounding marine area of Akkuyu NPP.

In this work, starting from these calculated activity concentrations and proper site-specific information (i.e., radiological coefficients for doses estimation, marine biota conversion factors, inhabitants' sea food consumption and marine occupancy), the doses received by representative marine organisms and the affected human population have been estimated. Moreover, environmental sensitivity analysis was carried out, considering the international authorities' recommendations and criteria of environmental protection, in order to reveal the most vulnerable features of the region and the main parameters controlling the radioecological processes.

## METHODOLOGY

### *Mathematical concept*

A basin-scale Mediterranean hydrodynamic model, based on the Princeton Ocean Model (POM)

---

\* Corresponding author: geoelefthe@hcmr.gr

and operational within POSEIDON forecasting system of the Hellenic Centre of Marine Research (HCMR), of  $1/20^\circ$  ( $\sim 5$  km) spatial resolution coupled with a Lagrangian dispersion Individual Based Model (IBM) has been developed, in order to simulate the dispersion of (dissolved and particulate) particles into the sea [13-14]. The processes controlling the particles' displacement included in the model are:

- Advection from ocean currents
- Waves Stokes drift
- Buoyancy/sinking (depending on the particles diameter/size and density)
- Random horizontal movement
- Random vertical movement (depending on turbulent vertical diffusion and waves)

while the computational scheme follows the concept of super-individuals that represent groups of particles sharing the same attributes. The position of each group is defined by the 3D displacement equations, produced by currents and waves:

$$x(t + dt) = x(t) + [u_c(x, y, z, t) + u_w(x, y, z, t)] \cdot dt + R_x, \quad (1)$$

$$y(t + dt) = y(t) + [v_c(x, y, z, t) + v_w(x, y, z, t)] \cdot dt + R_y, \quad (2)$$

$$z(t + dt) = z(t) + [w_c(x, y, z, t) + w_b] \cdot dt + R_z, \quad (3)$$

where  $u_c$ ,  $v_c$  and  $w_c$  are the three components of the ocean current velocity;  $u_w$ ,  $v_w$  are the wave Stokes drift velocity components (decreasing exponentially with the depth  $z$ ) and  $w_b$  the buoyancy velocity;  $R_x$ ,  $R_y$  and  $R_z$  represent the stochastic horizontal and vertical displacement.

In order to simulate the radionuclides dispersion in the marine environment, the additional processes of nuclear decay and particles' phase transfer have also been included into the model [7], following a stochastic approach where at each computational time step  $\Delta t$  a random number  $r$  between 0 and 1 is generated for each particle and it is compared with the probability  $p$  given by the equation:

$$p = 1 - e^{-a\Delta t}, \quad (4)$$

where, for the nuclear decay process,  $a$  is the radioactive decay constant  $\lambda$  of each radionuclide ( $\lambda = \ln 2/T_{1/2}$ , in  $s^{-1}$ ) and  $p$  the probability that the particle is removed from the computation (if  $r < p$ ), while for the phase transfer process,  $a$  represents the kinetic transfer coefficient  $k_i$  between the two phases ( $i = 1$  for dissolved to particulate and  $i = 2$  for particulate to dissolved, in  $s^{-1}$ ) and  $p$  the probability that the particle will actually change phase (again if  $r < p$ ). The  $k_i$  values for each element can be experimentally calculated and they were retrieved from the literature [9].

### Implementation

The hydrodynamic regime and the bathymetry of the study area are presented in Fig. 1. The Eastern Mediterranean basin has a complex morphology with depths greater than 4000 m, while the surface circulation is dominated by a series of semi-permanent currents and eddies. The main circulation features include the Atlantic Ionian Stream (AIS) that crosses the Ionian Sea, bordered by the Gulf of Syrte anticyclone to the southwest and the western Crete cyclone to the northeast. This stream continues as the Mid-Mediterranean Jet (MMJ) that crosses the Levantine basin with a cyclonic pathway, either deflected to the west of Cyprus during summer or continuing to the Lebanese and Syrian coasts to create the Cilician (CC) and Asia Minor (AMC) currents along the Turkish coast to the north. In parallel, an along-slope cyclonic Lyvio-Egyptian current (LEC) follows the southeast coastline up to the Syrian Coast, where it moves north. Rhodes gyre located at the South of Rhodes Island is the most important cyclonic feature, while a series of semi-permanent anticyclonic or recurrent cyclonic and anti-cyclonic eddies are also observed below the MMJ, the Ionian Sea and the South Aegean.

The Akkuyu NPP is located at the coastline of Mersin province in about 100 km from North Cyprus. The modelling scenario includes the accidental release of three radionuclides ( $^{137}\text{Cs}$ ,  $^{238}\text{Pu}$  and

$^{131}\text{I}$ ) commonly found after nuclear accidents, covering a wide range of radioactive half-lives and chemical properties. The release for each radionuclide is assumed to be an instant and uniform deposition at the sea surface (fall out) of 2000 TBq, in 70% dissolved and 30% particulate form, spread in a radius of 100 and 20 km, respectively, around the NPP. The 1<sup>st</sup> of January was set as the accident date, the hydrodynamic forcing was the multi-year (2014–2018) average of the region and the simulation period was one year, with calculation step the end of each month.

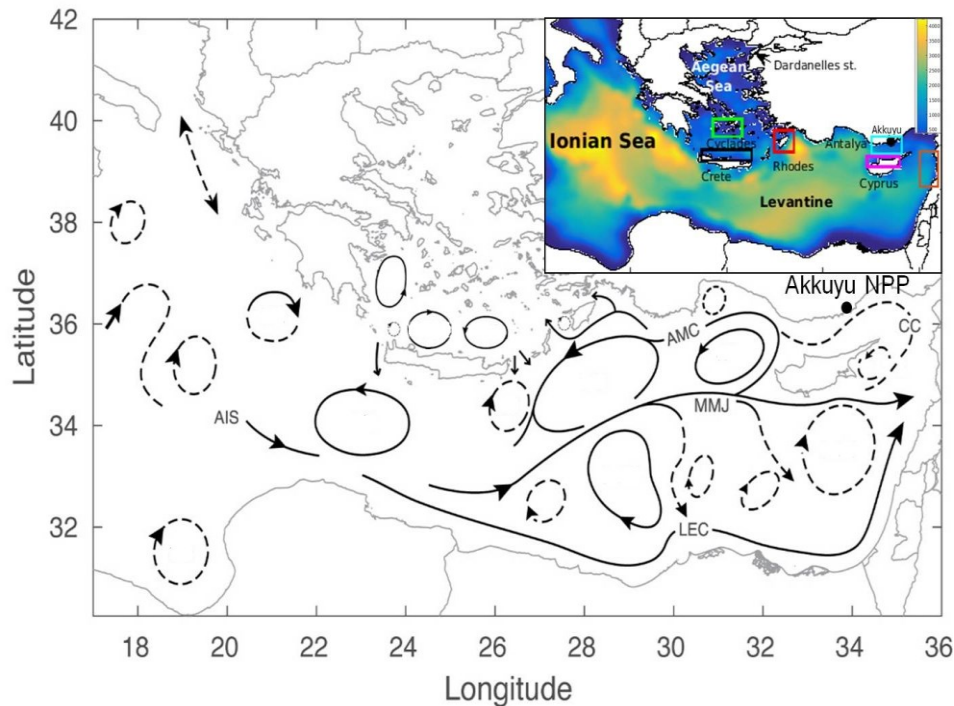


**Figure 1.** Surface circulation and bathymetry of Eastern Mediterranean (up right), along with the selected areas of interest (Akkuyu, N. Cyprus, Syrian coast, N. Crete, Rhodes and Cyclades). Transient upper thermocline features are depicted as dashed lines and the abbreviations are explained in the text.

## RESULTS AND DISCUSSION

### *Simulated dispersion*

The dispersion of the released radioactive plume into the marine environment for each radionuclide is presented in Fig. 2, as the average over the upper seawater layer (0–100 m).

For all three radionuclides, the dominant pathway of released plume has a westward direction, following the prevailing AMC current. However, the activity concentration of  $^{131}\text{I}$  is diminishing fast after the first month due to its relatively short half-life (8.03 d), while both  $^{137}\text{Cs}$  (30.05 y) and  $^{238}\text{Pu}$  (87.7 y) exhibit high concentrations, mainly at the coastal zone of Antalya and Rhodes Island. The notable similarity in the dispersion pattern and magnitude of dissolved  $^{238}\text{Pu}$  and  $^{137}\text{Cs}$  can be attributed to the slow sedimentation process (high depths and intense circulation), the constant contribution to the dissolved phase from the initial undissolved particles (faster particulate to dissolved phase transition for Cs) and the integration of concentrations at a relatively thick layer (0–100m) [15]. Moreover, a noticeable difference between these two radionuclides was found in the dispersion of the particulate phase [12, 15].

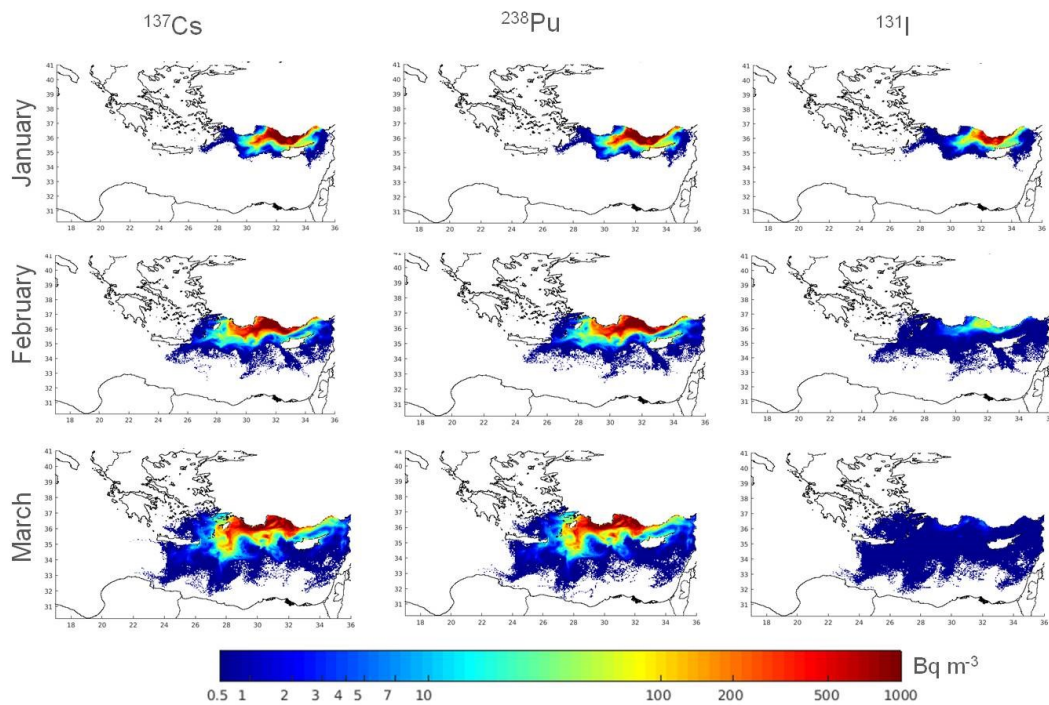


**Figure 2.** Average activity concentration (0-100 m) of dissolved  $^{137}\text{Cs}$ ,  $^{238}\text{Pu}$  and  $^{131}\text{I}$  during the first 3 months after the hypothetical accident at Akkuyu NPP.

### Impact assessment

In order to assess the effect of the released radiation to the environment, the doses to common marine biota (mammal, mollusc – bivalve, pelagic fish, phytoplankton and zooplankton) were calculated by applying the ERICA Tool [16]. The mean activity concentrations of the simulated radionuclides in the seawater at selected areas (see Fig. 1) were considered, while the default values of the conversion factors (dose conversion coefficient, concentration ratio and sediment-water distribution coefficient) were utilized, considering the internal, as well as the external exposure. As expected, the maximum dose rates were found during the first days in the region of Akkuyu with values varying from  $0.07 \text{ Gy h}^{-1}$  for pelagic fish and mollusc to  $0.3 \text{ Gy h}^{-1}$  for marine mammals and up to  $5000 \text{ Gy h}^{-1}$  for phytoplankton. However, after a year, the total doses in the regions of Rhodes were as much as 3.5 higher than the ones found in Akkuyu for all marine species, with values of approximately  $50 \text{ Gy y}^{-1}$  for mammals, fish and mollusc,  $250 \text{ Gy y}^{-1}$  for zooplankton and  $5 \text{ Gy y}^{-1}$  for phytoplankton. Concerning the contribution to the dose,  $^{238}\text{Pu}$  was the main contributor, especially for phytoplankton,  $^{137}\text{Cs}$  was the main contributor for mollusc, while the effect of  $^{131}\text{I}$  was very limited and only for the first month. Overall, even in Akkuyu where the radiation exposure diminished rapidly after the first month, the dose rates to all considered organisms were above the screening value of  $400 \mu\text{Gy h}^{-1}$  [17] even one year after the accident.

Based on the seawater activity concentration surrounding the most affected areas (see Fig. 2), the committed effective dose  $E$  (in  $\mu\text{Sv y}^{-1}$ ) from marine food consumption was calculated using the dose coefficients for intake of radionuclides by a representative adult according to the equation [18]:

$$E = \sum_i \sum_j A_i \cdot CR_{ij} c_j \cdot DCF_i, \quad (5)$$

where  $A_i$  is the seawater activity concentration for radionuclide  $i$  (in  $\text{Bq m}^{-3}$ ),  $CR_{ij}$  the concentration ratio for radionuclide  $i$  and marine biota  $j$  (in  $\text{m}^3 \text{ kg}^{-1}$  fresh weight),  $c_j$  is the annual sea food consumption of marine biota type  $j$  (in  $\text{kg y}^{-1}$ ) and  $DCF_i$  is the internal dose conversion factor for radionuclide  $i$  (in  $\text{Sv Bq}^{-1}$ ). The annual fish consumption for the Eastern Mediterranean population

was set to  $24 \text{ kg y}^{-1}$  per adult (85% fish, 10% mollusc, and 5% crustacean) [19], assuming that all of their food intake from the marine pathway comes from the local environment. The recommended by the radioprotection agencies values of CR [20] and DCF [18] were adopted.

The estimations of the effective dose evolution and the annual total dose received by a resident are presented in Fig. 3 for each of the examined regions. Considering that the estimated total ingestion exposure, depending on radionuclide composition of food and drinking water, ranges between  $200$  and  $800 \text{ } \mu\text{Sv y}^{-1}$  worldwide [17], the monthly doses rates in all sites, apart from the Akkuyu coast, eventually exceed the maximum natural ingestion exposure rate. For the total annual dose to an adult individual, Rhodes and Cyclades habitants are significantly exposed to additional radiation, while North Crete and the Syrian Coast are left practically unaffected.

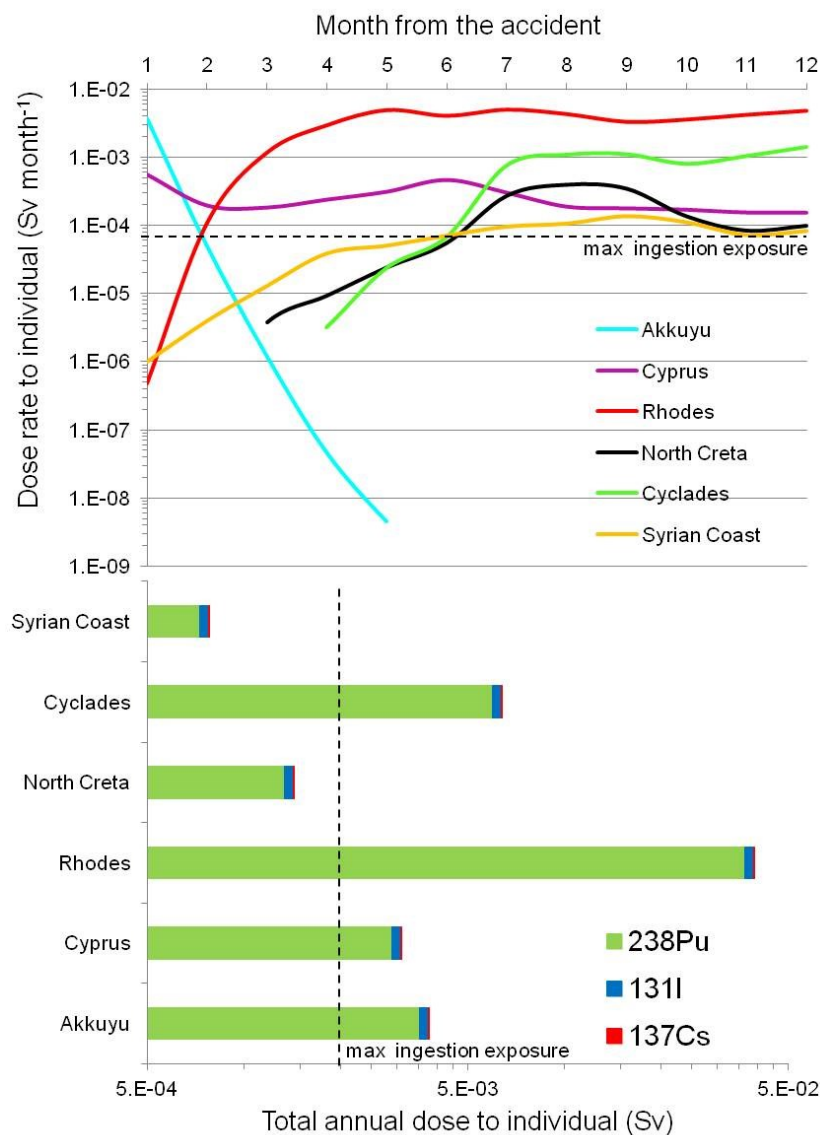


**Figure 3.** Monthly dose rate from all radionuclides (up) and total annual dose per nuclide (down) received by an adult habitant of each region due to sea food consumption from the local marine environment. Dash lines refer to the maximum natural ingestion exposure due to food and water consumption ( $66.7 \text{ } \mu\text{Sv month}^{-1}$  and  $800 \text{ } \mu\text{Sv year}^{-1}$ , respectively), according to UNSCEAR [17].

Another measure of the radiological impact on different regions is the environmental sensitivity [3]. Environmental sensitivity is the ratio of the effect to an environment for a given stress, thus it is



used to rank the environments according to their vulnerability. Table 1 presents the sensitivity index of selected marine areas, expressed as the final effect under the same stress according to the equation:

$$SI = \frac{\text{total annual dose to a representative adult habitant (Sv)}}{\text{initial radionuclide deposition (2000 TBq)}} \quad (6)$$

From the results it is derived that the selected areas can be classified to three groups of marine environments facing limited (North Crete, Syrian Coast), moderate (Akkuyu, Cyprus and Cyclades) and severe impact (Rhodes) for the contamination scenario.

**Table 1.** Environmental sensitivity ( $Sv Bq^{-1}$ ) based on the total annual dose to adult resident per initial deposition

Akkuyu	Cyprus	Rhodes	North Creta	Cyclades	Syrian Coast
19	16	195	7	32	4

## CONCLUSIONS

The installation of large nuclear facilities in coastal areas, such as nuclear power plants, can pose risk of serious contamination of the adjacent marine environment. For this reason, prior and during their operation, several actions must take place including the systematic control of radio-pollution in the surrounding compartments, the public awareness due to a potential nuclear accident and the support of State authorities for decision and mitigation of environmental crises adopting relevant EU and IAEA policies. To this end, a contamination scenario of accidental radionuclides dispersion to the Eastern Mediterranean Sea from the recently constructed Akkuyu NPP in South Turkey was performed applying radiomodel simulations. The main objectives were to estimate the radioecological impact to marine biota and human habitants, as well as to assess the environmental sensitivity for the optimization of marine monitoring/early warning networks design.

For the performed modelling exercise, it was found that:

- The radioactive plume has a predominant westward direction towards the neighboring coasts of Akkuyu, with maximum concentrations located at the marine areas around Rhodes and Kastelorizo islands, and Mersin and Antalya coasts.
- $^{238}\text{Pu}$  and  $^{137}\text{Cs}$  exhibit similar dispersion trends, while  $^{131}\text{I}$  dispersion is limited at the coastal area around the NPP.
- Marine biota and human habitants receive doses above the screening values, mainly attributed to  $^{238}\text{Pu}$ , even one year after the accident.
- Rhodos and Cyclades are the most vulnerable sites while the effect to the Akkuyu coastal area diminish rapidly.

Although the presented work provides an overall assessment of the impact of a hypothetical accident, additional information and developments are required in order to have more reliable estimations of a possible incident. Such improvements would include the study of the atmospheric effect in the initial fall out, as well as complementary scenarios of not instant depositions. Moreover, an effective management of radiological contamination in such a dynamic and wide environment as the Eastern Mediterranean Sea would include, apart from the model's optimization engaging all involved countries, the development of a monitoring network implementing proper international strategies.

## References

- [1] IAEA, TECDOC 1719, p. 156 (2013)
- [2] IAEA, BIOMASS 4, p. 332 (2003)
- [3] IAEA, TECDOC 1678, p. 50 (2012)
- [4] R. Perianez et al., Sci. Total Environ. 569/570, 594 (2016)

- [5] R. Perianez et al., *J. Environ. Radioact.* 198, 50 (2019)
- [6] J.A. Sanchez-Cabeza et al., *J. Mar. Syst.* 33, 457 (2002)
- [7] G. Eleftheriou et al., *Sci. Total Environ.* 533, 133 (2015)
- [8] R. Bezhenar, et al., *J. Environ. Radioact.* 208/209, 106023 (2019)
- [9] G. Eleftheriou and M. Iosjpe, *J. Environ. Radioact.* 222, 106360 (2020)
- [10] IAEA, PRIS database (2022) <https://pris.iaea.org/pris/>
- [11] C. Tsabaris et al., *Prog. Nucl. Energy* 139, 103879 (2021)
- [12] C. Tsabaris et al., *J. Environ. Radioact.* 251/252, 106964 (2022)
- [13] K.P. Tsiaras, *Ocean Dynam.* 67, 673 (2017)
- [14] A. Pollani et al., *Mar. Pollut. Bull.* 43, 270 (2001)
- [15] C. Tsabaris et al., *J. Environ. Radioact.* 255, 106994 (2022)
- [16] J.E. Brown et al., *J. Environ. Radioact.* 99, 1371 (2008)
- [17] UNSCEAR, *Sourc. Eff. Ioniz. Radiat.* Vol. 1 (2000)
- [18] ICRP, *Annal. ICRP* 119, Suppl. 41 (2012)
- [19] EUMOFA, *The EU fish market*, EC (2020)
- [20] IAEA, *TRS 479*, p. 211 (2014)